HHS Public Access

Author manuscript

J Am Soc Mass Spectrom. Author manuscript; available in PMC 2017 December 13.

Published in final edited form as:

J Am Soc Mass Spectrom. 2017 January ; 28(1): 29–37. doi:10.1007/s13361-016-1499-5.

Quantitation of the Noncovalent Cellular Retinol-Binding Protein, Type 1 Complex Through Native Mass Spectrometry

Wenjing Li, **Jianshi Yu**, and **Maureen A. Kane**

Department of Pharmaceutical Sciences, School of Pharmacy, University of Maryland, 20 N. Pine Street, Room 723, Baltimore, MD 21201, USA

Abstract

Native mass spectrometry (MS) has become a valuable tool in probing noncovalent protein–ligand interactions in a sample-efficient way, yet the quantitative application potential of native MS has not been fully explored. Cellular retinol binding protein, type I (CrbpI) chaperones retinol and retinal in the cell, protecting them from nonspecific oxidation and delivering them to biosynthesis enzymes where the bound (holo-) and unbound (apo-) forms of CrbpI exert distinct biological functions. Using nanoelectrospray, we developed a native MS assay for probing apo- and holo-CrbpI abundance to facilitate exploring their biological functions in retinoid metabolism and signaling. The methods were developed on two platforms, an Orbitrap-based Thermo Exactive and a Q-IMS-TOF-based Waters Synapt G2S, where similar ion behaviors under optimized conditions were observed. Overall, our results suggested that within the working range (~1–10 μM), gas-phase ions in the native state linearly correspond to solution concentration and relative ion intensities of the apo- and holo-protein ions can linearly respond to the solution ratios, suggesting native MS is a viable tool for relative quantitation in this system.

Graphical abstract

Correspondence to: Maureen A. Kane; mkane@rx.umaryland.edu.

Electronic supplementary material The online version of this article (doi:10. 1007/s13361-016-1499-5) contains supplementary material, which is available to authorized users.

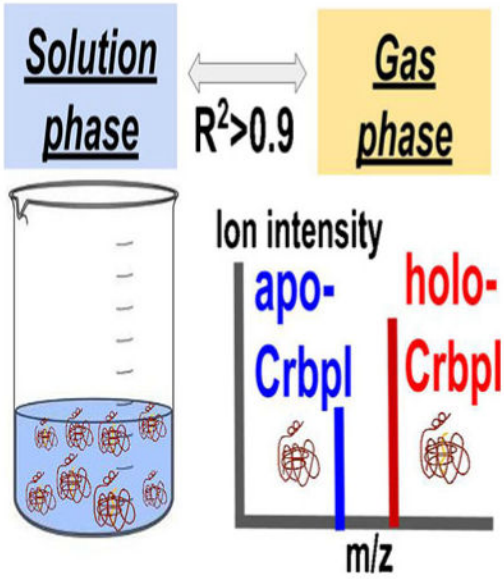

Keywords

Native mass spectrometry; Quantification; Noncovalent protein complex; Cellular retinol-binding protein; Vitamin A

Introduction

Since noncovalent protein–ligand complex was first observed in the mass spectrometer in 1991 [1], native mass spectrometry (native MS) has become a valuable tool in studying protein–ligand interactions, including their structures, binding affinities, and kinetic and thermodynamic parameters, which has proven to be superior to other traditional methods (isothermal titration calorimetry, surface plasmon resonance spectroscopy, nuclear magnetic resonance spectroscopy) in speed and sensitivity [2]. The term “native” implies physiological conformation is maintained throughout the gentle ESI process transferring intact molecules from solution phase to gas phase. Discussions continue as to what extent the interactions in the solution phase can be preserved in the gas phase [3–5]. Studies on various noncovalent complexes have exhibited a correlation of stoichiometry, binding affinity, and conformation between *in vacuo* and in solution [6–8]. Models that have been developed for understanding ion formation and the desolvation process under native conditions have also indicated the likely possibility of the retained structure of protein complexes [9]. These combined efforts have encouraged the application of native MS to study protein interactions with ligands, peptides, proteins, or nucleotides, and provided an avenue for timely and sample-efficient analysis. Of note, quantitative analysis by native MS has shown promise in monitoring single protein species for binding affinities or kinetics with small molecules [10–12]. Semi-quantitation for heterogeneous protein mixtures has been made possible through improved resolving power and algorithm innovations [13, 14], with advancements in coupling online or offline separation techniques [15–17]. However, the correlation between absolute ion response and concentration in solution for protein-complex

species requires further study because of the complexities in response factors, intrinsic interactive forces[10–12], and instrumental settings among the noncovalent complexes being investigated [3, 18–21]. This lack of knowledge has resulted in difficulties in comparing data from native MS with other methodologies [22, 23], hindering a comprehensive understanding of ion behavior under the native condition, which may result in an underestimation of the analytical power of this approach.

Cellular retinol binding protein, type I (CrbpI), is a chaperone protein that binds retinol and retinal 1:1 with high affinity (low nM *K'd*), protects its ligand from nonspecific oxidation, and influences the biosynthetic flux of retinol to its active metabolite, all-trans retinoic acid (atRA) [24, 25]. Holo-CrbpI (retinoid-bound form) serves as a substrate for both enzymes that produce active metabolite atRA and enzymes that esterify retinol for storage as retinyl esters. Apo-CrbpI (unbound form) has the regulatory ability to stimulate or inhibit the activity of specific enzymes [25]. The elegant role of CrbpI as a modulator of metabolite flux lies in the ratio of holo-CrbpI (bound form) and apo-CrbpI (unbound form) that directs intracellular retinol towards either atRA biosynthesis (active metabolite) or retinyl ester formation (storage) depending on whether vitamin A is in abundance or in demand. Previously, retinol and CrbpI were quantified separately in rat liver where CrbpI was quantified by radioimmunoassay and retinol was quantified by HPLC-UV [25, 26]. Here, CrbpI was in greater abundance than retinol, where CRBP and retinol concentrations were ~7 and ~5 μM, respectively [24, 26]. However, the physiological ratio in many extrahepatic tissues and the extent it fluctuates under conditions of vitamin A abundance, vitamin A demand, or CrbpI loss due to disease remains incompletely understood because of technical difficulty in directly quantifying apo- and holo-CrbpI from a complex matrix (*in vivo* source). This technical difficulty arises from CrbpI being a poor immunogen where traditional immunoassays reliant on specific antibodies have resulted in conflicting data among different research labs [27–29]. As such, the lack of antibodies with sufficient specificity means traditional antibody-based methods have not and will not be fully successful toward the characterization of the CrbpI complex. MS-based analyses can provide the detection specificity that antibody-based methods for CrbpI lack. Native MS provides the ability to interrogate the abundance of the apo-CrbpI and holo-CrbpI complex directly. A bottom-up proteomic approach could also provide specific detection of CrbpI abundance but would require a parallel analysis of CrbpI ligand [30–32] and then calculation of the amount of apo- and holo-CrbpI.

In recent years, the significance of CrbpI to maintaining retinoid homeostasis has been of increasing interest, given its epigenetic silencing occurrence in 10 of the top 12 most common cancers [33]. Additional studies have indicated that CrbpI loss is an early event in carcinogenesis that is associated with the increased propensity for cancer progression and the incidence of metastasis [34] in almost top 10 cancer types, indicating its crucial function as an indicator of local retinoid metabolism and a potential marker for cancer detection and treatment [33]. As such, the reliable measurement of holo- and apo-CrbpI abundance will facilitate a fundamental understanding of its biological role in retinoid signaling, and may also serve in determining CrbpI levels (both bound and unbound forms) as a molecular indicator of disease state that may provide diagnostic and prognostic value.

Here, for the first time, we developed a native mass spectrometric assay for measuring the abundance of apo-CrbpI and holo-CrbpI, and examined our results on two different platforms (Orbitrap-based Thermo Exactive and Q-IMS-TOF-based Waters Synapt G2S) to quantitatively investigate ion behavior under native conditions. This proof-of-concept study leads to a greater understanding of the native mass spectrometry of complex mixtures and informs on the behavior of small, noncovalent protein–ligand complexes in the mass spectrometer. Using CrbpI-retinol as a model system, we explored the working dynamic range where native mass spectrometry provides a linear correlation between ions in the gas phase and molecules in the solution phase, and took factors including concentration, solvent, and instrumental features into consideration on two widely adopted platforms. The results provided here on noncovalent protein complexes in the gas phase will contribute to the understanding of native mass spectrometry as a quantitative tool. Additionally, our assay demonstrates the potential for measurement of apo-/holo-CrbpI ratios *in vivo*, which will aid in the elucidation of retinoid homeostasis.

Experimental

Sample Preparation

Recombinant mouse CrbpI was prepared as previously described [35]. Briefly, mouse CrbpI with a GST tag was expressed recombinantly from *E. coli* cells. The GST tag was cleaved with Promega ProTEV protease (Promega, Madison, WI, USA). Purified protein was dialyzed through a 3 kDa molecular weight cutoff (MWCO) spin filter columns (Millipore, Billerica, MA, USA) and stored in PBS solution at −80 °C. All-*trans*-retinol was purchased from Sigma-Aldrich (St. Louis, MO, USA) and handled under yellow light. To make holo-CrbpI, retinol was dissolved in ethanol, and was added to apo-CrbpI solution with a glass Hamilton syringe (Sigma-Al-drich), gently mixed, and equilibrated for 5 min at room temperature before measuring the absorbance. Apo-CrbpI and holo-CrbpI concentrations were determined from UV absorbance using published molar extinction coefficient (ε) values [36]. For any purified protein containing amino acids with aromatic rings, they exhibit an absorbance maxima at 280 nm in solution; CrbpI alone in solution shows an absorption peak at 280 nm (A_{280}) with a molar extinction coefficient 28080 $M^{-1}cm^{-1}$. Retinol in ethanol shows an absorption peak at 325 nm; however, when retinol is bound to CrbpI, there is a 25 nm shift in λ_{max}, which yields a peak maximum for holo-CrbpI at 350 nm (A_{350}). The ε for retinol bound to CrbpI was previously determined to be 50200 $M^{-1}cm^{-1}$ [28]. Retinol binds to CrbpI in a 1:1 ratio where 100% binding yields a theoretical A_{350}/A_{280} ratio proportional to the ε ratio of retinol bound to CrbpI (50200 $M^{-1}cm^{-1}$)/CrbpI alone (28080 $M^{-1}cm^{-1}$), which is 1.8. An A_{350}/A_{280} ratio above 1.6 was required in these studies to ensure sufficient binding (>90%) between retinol and CrbpI.

Mass Spectrometry

Native MS mass spectra were acquired on two instruments for comparison: an Orbitrap-based instrument (Exactive; Thermo Fisher Scientific, Bremen, Germany) and a quadrupole-ion mobility separation-time-of-flight (Q-IMS-TOF) instrument (Synapt G2S; Waters, Manchester, UK). Before analysis, all protein sample solutions were buffer exchanged into 10 mM ammonium acetate using a 3 kDa cutoff centrifugal filter (Millipore). Samples were

adjusted to a solution concentration between 0.25 to 10 μM according to UV absorbance and then introduced to the gas phase by direct infusion using a syringe pump. Native-like cations were generated using nanoelectrospray ionization from a PicoTip emitter with a 30 μm internal diameter (New Objective, Woburn, MA, USA). A stable spray at nanoflow rate was obtained for 1 min for data analysis. All MS experiments were performed in positive ion mode and instrumental parameters were optimized on each instrument to minimize in-source dissociation as described. Myoglobin from equine skeletal muscle (Sigma-Aldrich, MO, USA) was tested as a native MS assay control and an internal standard in some studies at either 2 μM (Exactive) or 1 μM (Synapt) concentration as indicated in Figure Legends.

Exactive—The instrument was calibrated by Angiotensin II in the mass range (200–3000 Da). Operating pressures in the instrument were typically 1–2 mbar in the S-lens region, 3 $\times 10^{-9}$ mbar in the source chamber, and 5 $\times 10^{-11}$ mbar in the analyzer chamber. The conditions of the interface were as follows: flow rate 50 nL/min; electrospray voltage 1.5 kV; capillary voltage 40 V; tube-lens voltage: 120 V; skimmer voltage: 20 V; capillary temperature 40 °C. Mass spectra were acquired over the range m/z 1500–3000 and 50 to 80 scans were averaged prior to data analysis. MASH Suite was used for mass deconvolution and relative quantitation [37].

Synapt G2S—Full scan mass spectra were recorded in Resolution Mode where the experimental resolution that was achieved was at least 20,000 across samples. The typical operating conditions were optimized for the highest sensitivity of detection: flow rate, 100 nL/min; electrospray voltage, 2.5 kV; source temperature, 50 °C; trap CE, 2 V; gas control, 6 mL/min, cone voltage, 0 V. The backing pressure at the time of experiment was 3.0 mbar; trap pressure 1.5×10^{-4} mbar. Data for each sample was acquired for 1 min in the mass range between m/z 1000 and 3500. Mass calibration was performed using CsI. MassLynx V4.1 (Waters, Manchester, UK) was used for experimental mass determination and quantitation.

Quantitative Analysis

Quantitative measurements for native MS of both CrbpI and myoglobin included the abundance of all charge states under native conditions in the calculation for each species, where an integration of isotopic peak areas, including areas of adduct ions, were utilized for each charge state. Peak areas with peak scores below 90 (determined through MASH suite), which correlated to the ion intensities of those peaks being below 5% of the parent protein ion, were discarded.

The y-axes entitled “normalized absolute ion intensity” in Figure 2 were calculated through normalizing the absolute ion peak areas in order to allow for easier comparison between the two instruments. The “dissociation level” that is mentioned in the text refers to the peak area ratios of apo-CrbpI to the sum of apo- and holo-CrbpI.

Results and Discussion

Qualitative Characterization of CrbpI by Native MS

Exactive—As myoglobin has been widely studied as a model system for developing native MS assays and has a similar molecular weight and charge state distribution as CrbpI, we used it as a control to test the generalizability of the optimization for native conditions we developed for CrbpI. Under native conditions, myoglobin showed a charge state distribution that centered on 8+ as previously reported [38] (Figure 1ai), with an experimental monoisotopic mass of 17555.2 Da. The denatured myoglobin has a monoisotopic mass of 16940.5 Da (data not shown) suggesting the mass shift was due to the binding of heme. Under the same experimental settings, the native mass spectra of the complex of CrbpI bound to its ligand, retinol, displayed a mixture of a mixture of bound (holo-) and unbound (apo-) CrbpI showing two distinct ion series corresponding to apo-CrbpI with a monoisotopic mass of 16613.1 Da and 16899.4 Da for holo-CrbpI (Figure 1aii). This value is in excellent agreement with the theoretical mass calculated from the plasmid sequence of apo-CrbpI (16613.2 Da) and holo-CrbpI (16899.4 Da) with a mass difference of retinol (286.2 Da). As expected, under nondenaturing conditions, the compact structure of apo-CrpbI and holo-CrbpI shared similar charge state distribution that centered on 8+, likely due to their similar conformations according to previous NMR analysis [39].

As reported in the literature [39], the observation of intact noncovalent complexes during native MS analysis have been found to be particularly influenced by various interface parameters, which affect the reproducibility of native MS assays. With the utilization of a suitable commercialized emitter, we were able to reproduce our data and compare them between different platforms. Various parameters were optimized where source temperature, flow rate, and spray voltage appeared to be the most critical factors for controlling the sensitivity, resolution, and in-source dissociation of the protein complex (Supplemental Figure 1). The absorbance spectra suggests that the fraction of free (unbound) protein in solution is less than ~10%, whereas we observed ~26% apo-protein of total protein under optimized conditions, where the additional proportion of apo-protein was attributed to in-source dissociation of holo-CrbpI (Figure 1aii). Since previous studies have indicated that the response factors for apo-CrbpI and holo-CrbpI should be similar [3], the additional dissociation must occur in the gas phase. We investigated the occurrence rates and extent of dissociation further (*vide infra*).

Peaks corresponding to protonated holo-CrbpI, apo-CrbpI, and myoglobin ions are observed in the spectra (Figure 1aiii, 1biii). No myoglobin was detected to be complexed with retinol consistent with the previously well-characterized high affinity binding of CrbpI to retinol [24]. The addition of myo-globin to holo-CrbpI did not change the charge state distributions but the absolute ion abundance dropped 20% to 80% for each species (Supplemental Figure 2A), compared with having holo-CrbpI alone at the same concentration. This proved to be a common event across concentrations suggesting a competition mechanism of ion formation under native conditions, which will be addressed in detail in the following section.

Synapt G2S—Data comparable to that collected on the Exactive (Figure 1a) was collected on the Synapt G2S (Figure 1b). Upon deconvolution of the spectra for all three samples,

average masses of 16623.8 ± 0.3 Da, 16909.8± 0.1 Da, and 17565.5 ± 0.7 Da were obtained, which is in good agreement with the theoretical average masses for apo-CrbpI (16623.9 Da), holo-CrbpI (16910.4 Da), and myoglobin (17565.6 Da), respectively. Similar to the results on the Exactive, mass spectra of CrbpI acquired under native conditions on the Synapt G2S showed a distribution centered on +8 charge states (Figure 1bii), consistent with a folded protein conformation. Two series at the +7, +8, and +9 charge states were observed, corresponding to apo-CrbpI and holo-CrbpI (Figure 1bii). In the case of holo-CrpbI, the more mild values of interface parameters that could be achieved on the Synapt G2S were found to preserve the noncovalent complex, where a low intensity distribution of dissociated holo-CrbpI was also observed (~39%). Also on the Synapt G2S, the addition of myoglobin to holo-CrbpI did not change the charge state distributions and had less of an impact on absolute ion abundance than on the Exactive for each species (Supplemental Figure 2B) compared with having holo-CrbpI alone at the same concentration under the same instrumental conditions.

Evaluation of the CrbpI Complex Stability in the Gas Phase

(1) Charge State Distribution for the CrbpI Complex—As shown in Figure 1, the charge state distribution showed a similar pattern on both instrument platforms investigated here. Figure 1 shows that 88% ± 5% of the signal originates from the +8 charge state among three different experimental component systems. The CrbpI complex with retinol does not result in a major change the observed charge-state distribution compared with apo-CrbpI. The charge state 8+ being the dominant species fits in well with the Rayleigh/CRM framework that is proposed elsewhere [9], supporting the existence of similar charge-state distributions for the apo- and holo-protein is a similar ion mobility drift time as detected using the Synapt G2S, which indicates a similar conformational shape [39, 40] (Supplemental Figure 3).

However, some subtle differences between apo-CrbpI and holo-CrbpI can be observed. The absolute ion intensity ratio of apo-CrbpI to holo-CrbpI increases as the charge state decreases from +9 to +7. For example, in Figure 1aii, at the +9 charge state, the ratio of apo-protein ion intensity to holo-protein ion intensity was found to be 61%, which is lower than 71% and 80% at the +8 and +7 charge states, respectively. Similarly, there were no significant differences between ion intensities at +8 and +7 charge states on Synapt, but charge state +9 showed lower ratios of free protein. For quantitative purposes, we combined the ion intensities of the three observed charge states since each ion species represents a quantifiable amount of molecule in the gas phase regardless of the charges that they carry.

(2) Preservation of CrbpI Complex Through Cooling Agent—We evaluated additional strategies to minimize dissociation during native MS methods to preserve the binding of a retinol to CrbpI. This 15 kDa protein contains 135 residues, which form two 5-stranded β-sheets [40]. The two β-sheets are packed orthogonally to form a solvent-filled β-barrel. The ligand-binding pocket, which physiologically accommodates all-*trans* retinol, is located inside the barrel. Importantly, the retinol binds CrbpI predominantly by hydrophobic interactions, as the ligand forms a hydrogen bond with the carbonyl group of the Gln 108 side chain. The experimental challenge often posed by small hydrophobic ligands is their

facile dissociation from proteins in the gas phase [41]. The removal of solvent molecules from the protein–ligand complex environment reduces the entropy-driven hydrophobic interactions to short-range van der Waals interactions. As a result, even very mild desorption conditions often cause partial or complete complex dissociation [3], thus compromising the ability to interrogate protein–ligand complexes by native MS. One strategy for stabilizing holo-CrbpI was to introduce imidazole into solution [10]. We utilized the ion peak area ratios of apo-CrbpI to total CrbpI as the dissociation level shown in Supplemental Figure 4. Addition of imidazole yielded a minor increase of the complex preservation (~5%); however, the loss in sensitivity and deterioration in peak shape were not worth the minor increase in complex preservation. Additional data on the impact of source conditions on dissociation level are included in Supplemental Figure 1.

(3) Concentration Dependence of In-Source Dissociation—We investigated the relationship between absolute gas-phase abundance and solution-phase concentration to determine if the linearity of response and the dissociation ratio would remain constant across concentrations. The response for apo-CrbpI and holo-CrbpI via native MS was compared with experimentally derived values from absorbance spectroscopy. As shown in Table 1, ion intensity of myoglobin is positively correlated with solution concentration (2–8 μM), and showed a good linear correlation R^2 (0.98) (Supplemental Figure 5). Saturation of signal and nonlinearity began at >8 μM and >6 μM on the Exactive and Synapt G2S, respectively. Holo-CrbpI showed a similar trend; however, the linear correlation was slightly less at R^2 (0.94) (Supplemental Figure 5). The relative intensity ratios of apo- to holo-CrbpI exhibited an inverse trend with increasing solution concentration (Figure 2a).

With the addition of an equal amount of myoglobin (2 μM) to the same concentration series of holo-CrbpI to serve as an internal standard, we observed an additional minor reduction in correlation R^2 (0.92). The same three systems were examined on the Synapt G2S and showed a similar decreasing trend in linear correlation (R^2) from single to two and three components (Figure 2b and Supplemental Figure 5). The loss of linear correlation among three different systems could possibly be explained by (1) additional variability introduced by the dissociation of holo-CrbpI that varies with concentration (Figure 2 and Supplemental Figure 5), and/or (2) fluctuations of myoglobin abundance in the gas phase due to the interaction at the ion formation stage where the competition of ions at different concentrations may result in differences in ion efficiency (Figure 2aiii, 2biii). Regardless of this observed variability, it is still possible for native MS to achieve linear gas-phase response as a function of solution concentration with $R^2 > 0.9$ with optimized instrumental parameters, solvents systems, and a good understanding of intrinsic protein complex characteristics.

(4) Impact of Additional Species on In-Source Dissociation—Previously, including an internal standard had improved the reproducibility of native MS assays [42]. Figures 2 and 3 show an effect on the retention of the holo-CrbpI complex when an additional species (myoglobin) is present. At lower concentrations of holo-CrbpI, when ion intensities of holo-CrbpI were lower than myoglobin, the in-source dissociation increased 16% compared with when holo-CrbpI was analyzed alone (Figure 3, on Synapt G2S). When

the signal intensity of holo-CrbpI was in excess of myoglobin (as is the case when both myoglobin and holo-CrbpI are present at 1 μM), the retention of holo-CrbpI was greatly improved, yet the spectrum of holo-CrbpI still exhibited ~5% more dissociation compared with analyzing holo-CrbpI alone. Whereas the mechanism of this concentration dependent dissociation warrants further study, potential mechanisms may include competition during ion formation that may alter ionization efficiencies for apo-CrbpI and holo-CrbpI.

Relative Quantitation of apo-/holo-CrbpI

In order to determine if we could use this native MS assay to probe the ratio of apo-/holo-CrbpI in solution, we defined the relationship between ion signal and solution concentration (Equation 1 and Equation 2). The factor relating the ion signal and the analyte concentration is called the electrospray response factor R. In this case, we also have to account for the dissociation ratio D, which also tended to vary across concentrations. The relative abundance of apo-CrbpI([P]) to holo-CrbpI([PL]) in the gas phase can be presented in the following equation:

$$\frac{[P]}{[PL]}=\frac{R_P(C_P+DC_{PL})}{R_{PL}(C_{PL}-DC_{PL})} \quad (1)$$

In Equation 1, C_P and C_{PL} represent the solution concentration of apo-CrpbI and holo-CrbpI. R_P and R_{PL} refer to the response factor for apo- and holo-CrbpI. Equation 1 can also be transformed in the following format:

$$\frac{[P]}{[PL]}=\frac{R_P}{R_{PL}(1-D)}*\frac{C_P}{C_{PL}}+\frac{R_P}{R_{PL}}*\frac{D}{1-D} \quad (2)$$

Equation 2 indicates that if R_P and R_{PL} could remain constant, and the dissociation ratio D only fluctuates at negligible level within the tested concentration range, the relative ion abundance in the gas phase could correlate with relative solution concentration in a linear pattern. The slope and intercept could inform on differences between instruments in terms of the relative response factor Rr(R_P/R_{PL}) and an average value of the dissociation ratio.

To test our theory, we kept apo-CrbpI constant (5 μM for Exactive, 2 μM for Synapt G2S), combined with a series of concentrations (from 0.1- to 1-fold excess of apo-CrbpI concentration) of retinol and allowed to equilibrate at room temperature for at least 5 min prior to native MS analysis (Figure 4). Table 2 shows excellent linear correlation on each platform, although each platform had a unique slope, intercept values, and linear equations. The difference of linear correlation parameters on two instruments indicates there may be a different selection process of ion transfer that possibly occurs both at the interface and in the mass spectrometer for apo- and holo-CrbpI. Previous studies have hypothesized that if the ligand is small, a protein and its complex should share the same R value across the concentration for native MS assays [12, 41, 43], which does not seem to hold true for the small protein that we studied here (as illustrated in Supplemental Figure 2). This finding may help researchers design better affinity studies or models for native MS methodologies.

Conclusion

In this proof-of-concept study, we developed methodology for relative quantitation for small protein and its ligand-bound form, apo- and holo-CrbpI, which provided sufficient accuracy and relevant sensitivity for potential future application to functional investigations of the role of CrbpI in retinoid metabolism and signaling. For this quantitative MS assay, we were able to obtain linear correlations between gas-phase ion abundance ratios and solution concentration ratios on two instruments, indicating this has the potential to become a translatable assay between instrument platforms and reproducible regardless of mass spectrometer design. The difference between response factors and in-source dissociation ratios that were observed in our native MS analyses indicated these crucial parameters need to be addressed in study designs and data analysis regarding to protein–ligand interactions. Moreover, to apply this assay for samples with complex backgrounds, appropriate separation strategies, including but not limited to hydrophobic interaction chromatography and size exclusion chromatography, will have to be integrated in the workflow either online or offline, which have shown promise for many protein complexes. Current studies in our laboratory are seeking to test the utility of this assay to determine the physiological ratio of apo-/holo-CrbpI in various tissues and cell types and how loss of CrbpI impacts this ratio and the corresponding metabolite flux.

Supplementary Material

Refer to Web version on PubMed Central for supplementary material.

Acknowledgments

This project was funded with federal funds from NIH: R01HD077260 and NIH/NIAID contract no. HHSN272201000046C. Additional support was provided by the University of Maryland, School of Pharmacy, Mass Spectrometry Center (SOP1841-IQB2014). The authors thank Dr. Jace Jones and Dr. Claire Carter for their discussions and contributions.

References

1. Ganem B, Li YT, Henion JD. Detection of noncovalent receptor-ligand complexes by mass spectrometry. J Am Chem Soc. 1991; 113:6294–9296.
2. Hilton GR, Benesch JLP. Two decades of studying noncovalent bio-molecular assemblies by means of electrospray ionization mass spectrometry. J R Soc Interface. 2012; 9:801–816. [PubMed: 22319100]
3. Kitova EN, Amr EH, Schnier PD, Klassen JS. Reliable determinations of protein–ligand interactions by direct ESI-MS measurements. Are we there yet? J Am Soc Mass Spectrom. 2012; 23:431–441. [PubMed: 22270873]
4. van Duijn E. Current limitations in native mass spectrometry based structural biology. J Am Soc Mass Spectrom. 2010; 21:971–978. [PubMed: 20116282]
5. Jurneczko E, Barran PE. How useful is ion mobility mass spectrometry for structural biology? The relationship between protein crystal structures and their collision cross sections in the gas phase. Analyst. 2011; 136:20–28. [PubMed: 20820495]
6. van den Heuvel RHH, Heck AJR. Native protein mass spectrometry: from intact oligomers to functional machineries. Curr Opin Chem Biol. 2004; 8:519–526. [PubMed: 15450495]
7. Benesch JLP, Ruotolo BT. Mass spectrometry: come of age for structural and dynamical biology. Curr Opin Struct Biol. 2011; 21:641–649. [PubMed: 21880480]

8. Gülbakan B, Basri G, Konstantin B, Renato Z. Determination of thermodynamic and kinetic properties of biomolecules by mass spectrometry. Curr Opin Biotechnol. 2015; 31:65–72. [PubMed: 25173612]
9. McAllister RG, Metwally H, Sun Y, Konermann L. Release of native-like Gaseous proteins from electrospray droplets via the charged residue mechanism: insights from molecular dynamics simulations. J Am Chem Soc. 2015; 137:12667–12676. [PubMed: 26325619]
10. Sun J, Jiangxiao S, Kitova EN, Klassen JS. Method for stabilizing protein-ligand complexes in nanoelectrospray ionization mass spectrometry. Anal Chem. 2007; 79:416–425. [PubMed: 17222003]
11. Zhang S, Van Pelt CK, Wilson DB. Quantitative determination of noncovalent binding interactions using automated nanoelectrospray mass spectrometry. Anal Chem. 2003; 75:3010–3018. [PubMed: 12964745]
12. Wortmann A, Arno W, Jecklin MC, David T, Martin B, Renato Z. Binding constant determination of high-affinity protein–ligand complexes by electrospray ionization mass spectrometry and ligand competition. J Mass Spectrom. 2008; 43:600–608. [PubMed: 18074334]
13. Ebong IO, Morgner N, Zhou M, Saraiva MA, Daturpalli S, Jackson SE, Robinson CV. Heterogeneity and dynamics in the assembly of the heat shock protein 90 chaperone complexes. Proc Natl Acad Sci USA. 2011; 108:17939–17944. [PubMed: 22011577]
14. Thompson NJ, Hendriks LJA, de Kruif J, Throsby M, Heck AJR. Complex mixtures of antibodies generated from a single production qualitatively and quantitatively evaluated by native Orbitrap mass spectrometry. MAbs. 2014; 6:197–203. [PubMed: 24351421]
15. Chen B, Bifan C, Ying P, Valeja SG, Lichen X, Alpert AJ, Ying G. Online hydrophobic interaction chromatography-mass spectrometry for top-down proteomics. Anal Chem. 2016; 88:1885–1891. [PubMed: 26729044]
16. Haberger M, Heidenreich AK, Schlothauer T, Hook M, Gassner J, Bomans K, Yegres M, Zwick A, Zimmermann B, Wegele H, Bonnington L, Reusch D, Bulau P. Functional assessment of antibody oxidation by native mass spectrometry. MAbs. 2015; 7:891–900. [PubMed: 26000623]
17. Woodard J, Jonathan W, Hollis L, Latypov RF. Nondenaturing size-exclusion chromatography-mass spectrometry to measure stress-induced aggregation in a complex mixture of monoclonal antibodies. Anal Chem. 2013; 85:6429–6436. [PubMed: 23742703]
18. Gavriilidou AFM, Basri G, Renato Z. Influence of ammonium acetate concentration on receptor–ligand binding affinities measured by native nano ESI-MS: A systematic study. Anal Chem. 2015; 87:10378–10384. [PubMed: 26399292]
19. Lin H, Hong L, Kitova EN, Klassen JS. Quantifying protein–ligand interactions by direct electrospray ionization-MS analysis: evidence of nonuniform response factors induced by high molecular weight molecules and complexes. Anal Chem. 2013; 85:8919–8922. [PubMed: 24044528]
20. Gabelica V, Galic N, Rosu F, Houssier C, De Pauw E. Influence of response factors on determining equilibrium association constants of non-covalent complexes by electrospray ionization mass spectrometry. J Mass Spectrom. 2003; 38:491–501. [PubMed: 12794869]
21. Chitta RK, Rempel DL, Gross ML. Determination of affinity constants and response factors of the noncovalent dimer of gramicidin by electrospray ionization mass spectrometry and mathematical modeling. J Am Soc Mass Spectrom. 2005; 16:1031–1038. [PubMed: 15914025]
22. Kuprowski MC, Lars K. Signal response of coexisting protein conformers in electrospray mass spectrometry. Anal Chem. 2007; 79:2499–2506. [PubMed: 17288464]
23. Kebarle P, Verkerk UH. Electrospray: from ions in solution to ions in the gas phase, what we know now. Mass Spectrom Rev. 2009; 28:898–917. [PubMed: 19551695]
24. Napoli JL. Interactions of retinoid binding proteins and enzymes in retinoid metabolism. Biochim Biophys Acta. 1999; 1440:139–162. [PubMed: 10521699]
25. Napoli JL. Physiological insights into all-trans-retinoic acid biosynthesis. Biochim Biophys Acta. 2012; 1821:152–167. [PubMed: 21621639]
26. Harrison EH, Blaner WS, Goodman DS, Ross AC. Subcellular localization of retinoids, retinoid-binding proteins, and acyl-CoA:retinol acyltransferase in rat liver. J Lipid Res. 1987; 28:973–981. [PubMed: 3668391]

27. Ong D, David O, Frank C. [34] Purification of cellular retinol and retinoic acid-binding proteins from rat tissue. Method Enzymol. 1980; 67:288–296.
28. Adachi N, Smith JE, Sklan D, Goodman DS. Radioimmunoas-say studies of the tissue distribution and subcellular localization of cellular retinol-binding protein in rats. J Biol Chem. 1981; 256:9471–9476. [PubMed: 6169711]
29. Levin MS, Li E, Ong DE, Gordon JI. Comparison of the tissue-specific expression and developmental regulation of two closely linked rodent genes encoding cytosolic retinol-binding proteins. J Biol Chem. 1987; 262:7118–7124. [PubMed: 3584109]
30. Jones JW, Pierzchalski K, Yu J, Kane MA. Use of fast HPLC multiple reaction monitoring cubed for endogenous retinoic acid quantification in complex matrices. Anal Chem. 2015; 87:3222–3230. [PubMed: 25704261]
31. Kane MA, Napoli JL. Quantification of endogenous retinoids. Methods Mol Biol. 2010; 652:1–54. [PubMed: 20552420]
32. Kane MA, Folias AE, Napoli JL. HPLC/UV quantitation of retinal, retinol, and retinyl esters in serum and tissues. Anal Biochem. 2008; 378:71–79. [PubMed: 18410739]
33. Esteller M, Guo M, Moreno V, Peinado MA, Capella G, Galm O, Baylin SB, Herman JG. Hypermethylation-associated Inactivation of the cellular retinol-binding-protein 1 Gene in human cancer. Cancer Res. 2002; 62:5902–5905. [PubMed: 12384555]
34. Farias EF, Ong DE, Ghyselinck NB, Nakajo S, Kuppumbatti YS, Miray Lopez R. Cellular retinol-binding protein I, a regulator of breast epithelial retinoic acid receptor activity, cell differentiation, and tumorigenicity. J Natl Cancer Institute. 2005; 97:21–29.
35. Pierzchalski K, Yu J, Norman V, Kane MA. CrbpI regulates mammary retinoic acid homeostasis and the mammary microenvironment. FASEB J. 2013; 27:1904–1916. [PubMed: 23362116]
36. Penzes P, Napoli JL. Holo-cellular retinol-binding protein: distinction of ligand-binding affinity from efficiency as substrate in retinal biosynthesis. Biochemistry. 1999; 38:2088–2093. [PubMed: 10026291]
37. Guner H, Close PL, Cai W, Zhang H, Peng Y, Gregorich ZR, Ge Y. MASH Suite: a user-friendly and versatile software interface for high-resolution mass spectrometry data interpretation and visualization. J Am Soc Mass Spectrom. 2014; 25:464–470. [PubMed: 24385400]
38. Li YT, Hsieh YL, Henion JD, Ganem B. Studies on heme binding in myoglobin, hemoglobin, and cytochrome *c* by ion spray mass spectrometry. J Am Soc Mass Spectrom. 1993; 4:631–637. [PubMed: 24227666]
39. Mittag T, Franzoni L, Cavazzini D, Schaffhausen B, Rossi GL, Günther UL. Retinol modulates site-specific mobility of apo-cellular retinol-binding protein to promote ligand binding. J Am Chem Soc. 2006; 128:9844–9848. [PubMed: 16866541]
40. Cowan SW, Newcomer ME, Jones TA. Crystallographic studies on a family of cellular lipophilic transport proteins. Refinement of P2 myelin protein and the structure determination and refinement of cellular retinol-binding protein in complex with all-trans-retinol. J Mol Biol. 1993; 230:1225–1246. [PubMed: 7683727]
41. Liu L, Kitova EN, Klassen JS. Quantifying protein-fatty acid interactions using electrospray ionization mass spectrometry. J Am Soc Mass Spectrom. 2011; 22:310–318. [PubMed: 21472590]
42. Gabelica V, Rosu F, De Pauw E. A simple method to determine electrospray response factors of noncovalent complexes. Anal Chem. 2009; 81:6708–6715. [PubMed: 19601639]
43. El-Hawiet A, Kitova EN, Arutyunov D, Simpson DJ, Szymanski CM, Klassen JS. Quantifying ligand binding to large protein complexes using electrospray ionization mass spectrometry. Anal Chem. 2012; 84:3867–3870. [PubMed: 22507285]

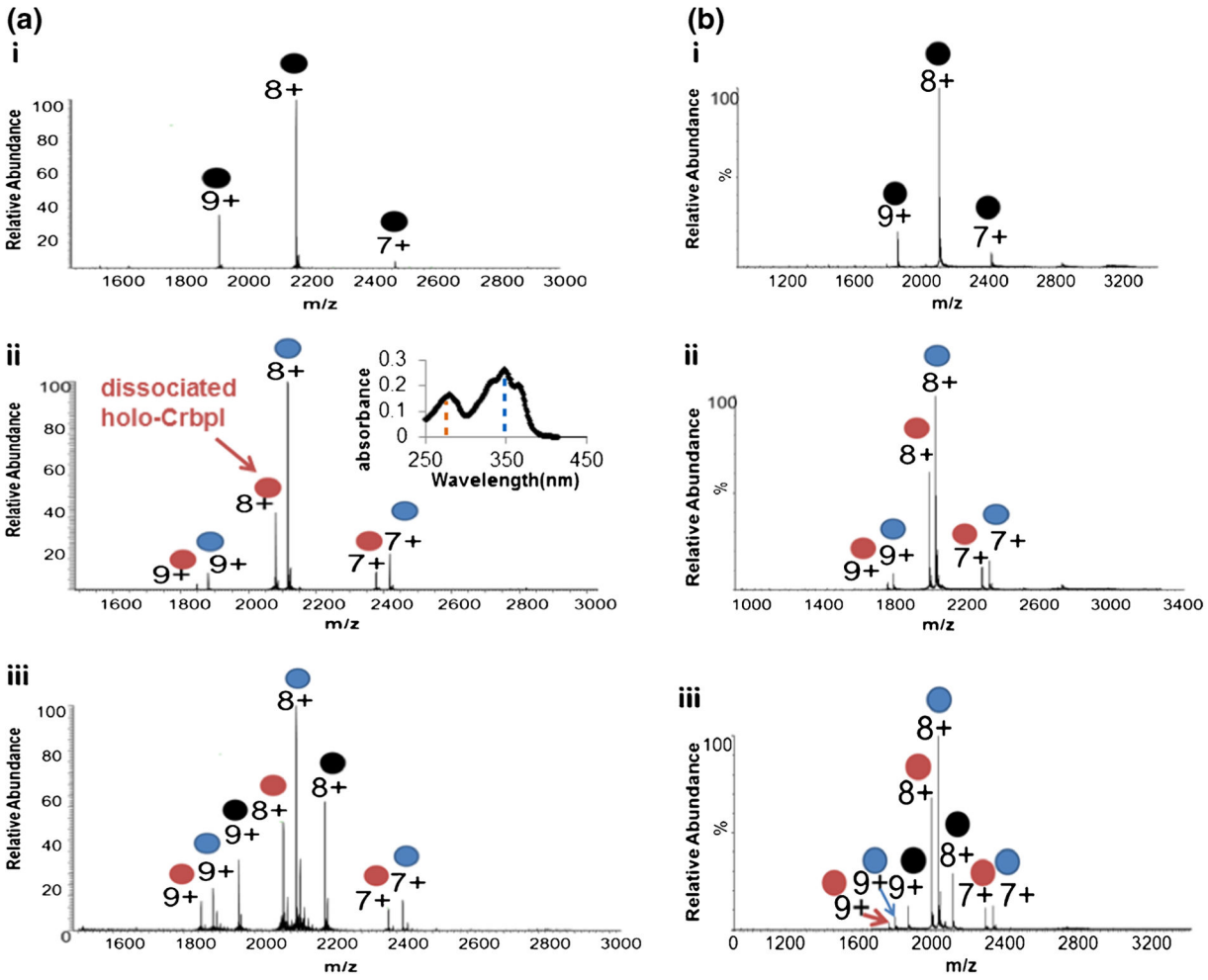

Figure 1.

Native mass spectra of (i) myoglobin (5 μM), (ii) holo-CrbpI (5 μM) with in-source dissociation (inserted figure represents UV spectra corresponding to holo-CrbpI in solution, A_{350}/A_{280} >1.6 were achieved to ensure more than 90% retinol were bound to CrbpI), (iii) holo-CrbpI (1 μM) with myoglobin (1 μM) on two instruments: (**a**) Exactive, (**b**) Synapt G2S. (myoglobin ●, holo-CrbpI ●, apo-CrbpI ●). Note: Holo-CrbpI forms a 1:1 complex with retinol

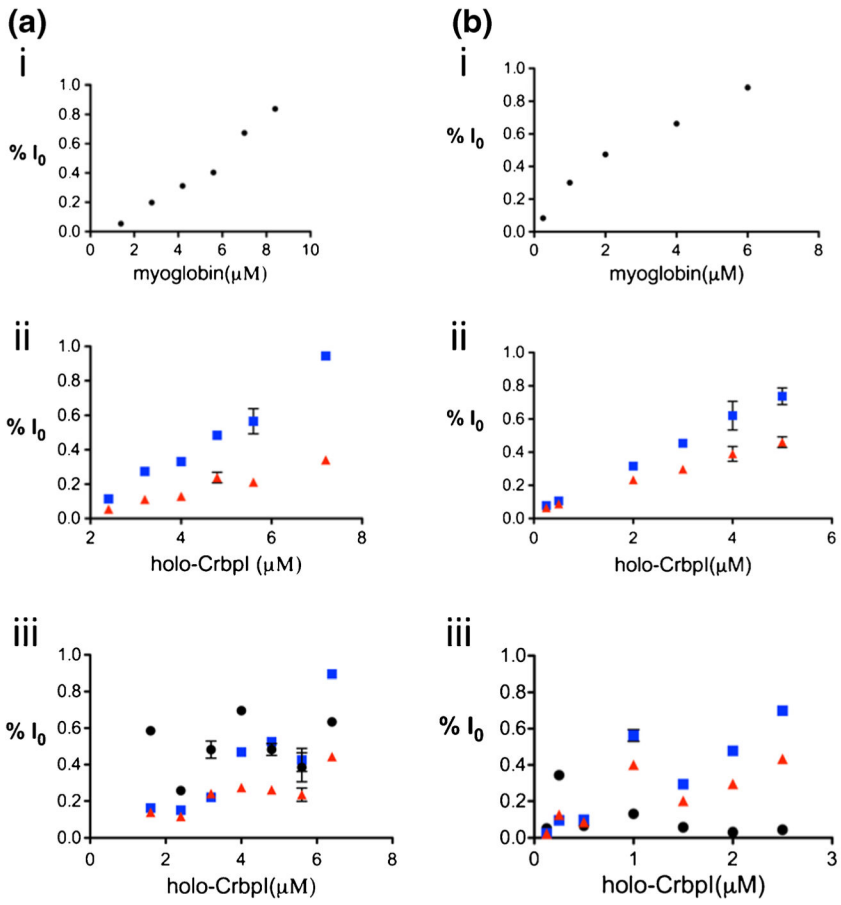

Figure 2.

Correlation of solution concentrations with normalized absolute ion intensities on two instruments (**a**) Exactive, (**b**) Synapt G2S. Results were obtained for three systems: (i) myoglobin, (ii) holo-CrbpI, (iii) holo-CrbpI spiked with a fixed concentration of myoglobin (2 μM for Exactive, 1 μM for Synapt). (myoglobin ●, holo-CrbpI ■, and apo-CrbpI ▲)

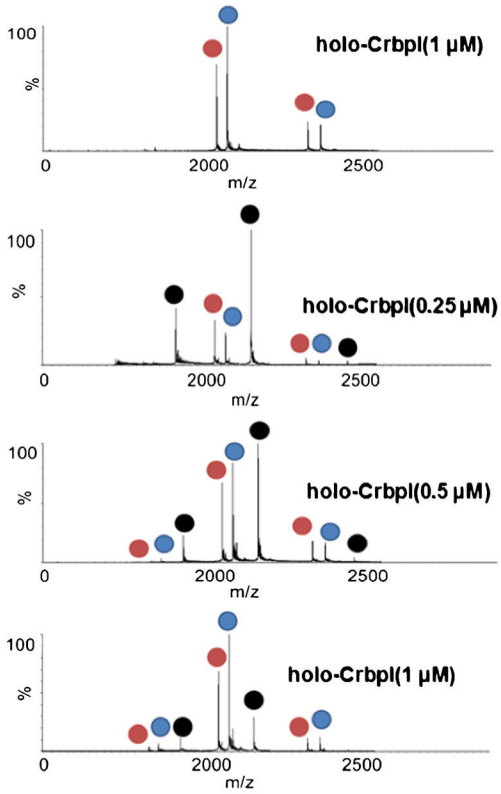

Figure 3.

Native mass spectra of holo-CrbpI with or without 1 μM myoglobin acquired on Synapt G2S (myoglobin ●, holo-Crbp I ●, apo-Crbp I ●)

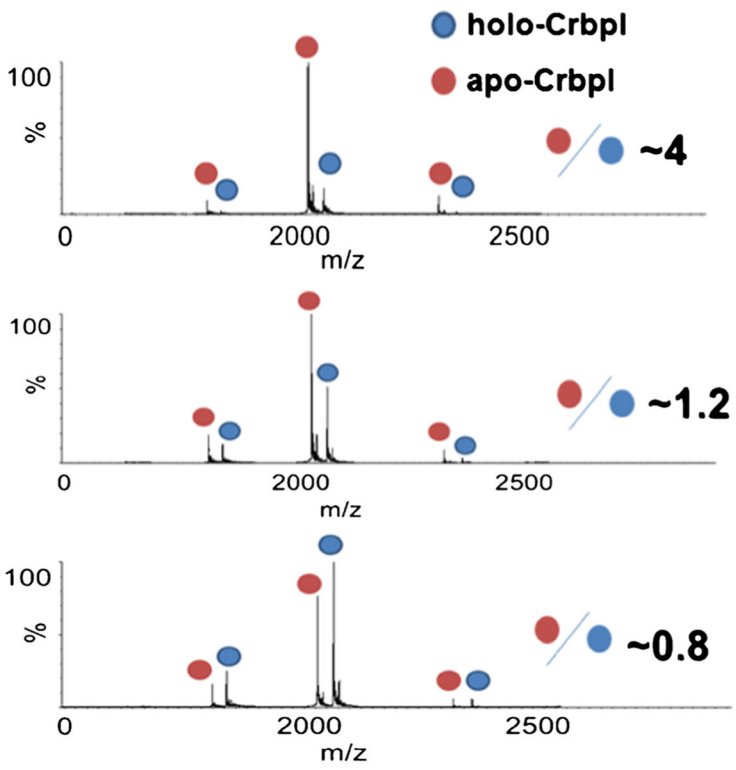

Figure 4.

Native mass spectra of CrbpI with different ratios of apo- to holo-forms acquired on Synapt G2S. The total concentration of CrbpI was fixed at 5 μM. Numbers shown in the figure represent the ratios of apo- to holo-CrbpI in solution, which were obtained through UV spectroscopy. The ligand retinol forms a 1:1 complex with CrbpI thus presented in an equivalent amount as holo-CrbpI

Table 1

Linear Correlations Between Solution Concentration and Ion Intensities Compared with Two Instruments*

	Exactive			Synapt		
	i	**ii**	**iii**	**i**	**ii**	**iii**
R^2	0.9732	0.9492	0.9262	0.9570	0.9419	0.9009
Linear Range (μM)	1.6–8	2.0–8	1.6–7	0.25–6	0.25–5	0.125–3

*Studies were categorized to i) myoglobin, ii) holo-CrbpI, iii) holo-CrbpI, spiked in with a fixed concentration of myoglobin (2 μM for Exactive, 1 μM for Synapt)

Table 2

Calculated Linear Regression of apo- to holo-CrbpI Ratios in the Solution Phase and Gas Phase

	Exactive	**Synapt**
Slope	1.148 ± 0.022	1.652 ± 0.040
Intercept	0.434 ± 0.067	0.083 ± 0.158
R^2	0.9941	0.9839
Experimental ratio range (apo/holo)	0.27–6.67	0.14–7.14